Supplemental Material for Fermi arc induced vortex structure in Weyl beam shifts

Udvas Chattopadhyay,[1] Li-kun Shi,[2] Baile Zhang,[1,3] Justin C. W. Song,[1,2] and Y. D. Chong[1]

[1] *Division of Physics and Applied Physics, School of Physical and Mathematical Sciences, Nanyang Technological University, Singapore 637371, Singapore*

[2] *Institute of High Performance Computing, A*STAR, Singapore 138632, Singapore*

[3] *Centre for Disruptive Photonic Technologies, Nanyang Technological University, Singapore 637371, Singapore*

In this supplement, we discuss the winding behavior of the planar reflection coefficient ϕ; derive analytical formulas for the shift of Gaussian beams in a Weyl medium, and compare them to numerical results; derive the eigenvectors, reflection coefficients, and beam shifts in the quadratic Hamiltonian model; and derive the accumulation of beam shifts in a thin film geometry. Unless otherwise specified, it is assumed that $v = 1$ and that θ_b is a constant.

A. Reflection phase winding around Fermi arc touching-point

As mentioned in the main text, the non-trivial behaviour of the reflection phase near the Fermi arc touching-point can be understood by considering the limiting case $k_z^\pm \to 0$. For $k_z^\pm = 0$, the incident and reflected waves are linearly dependent and the total (envelope) wavefunction is

$$\psi_{\text{tot}} = \frac{1}{\sqrt{2}}(1 + e^{i\phi}) \begin{bmatrix} 1 \\ e^{i\alpha} \end{bmatrix}. \tag{S1}$$

The boundary condition (Eq. 3 of main text) then implies

$$(1 + e^{i\phi})(1 + e^{i(\alpha - \theta_b)}) = 0, \tag{S2}$$

which can be satisfied by (i) $\phi = \pi$ and (ii) $\alpha - \theta_b = \pi \pmod{2\pi}$. Fig. S1 shows ϕ as a function of α parametrizing circular patches of different radius close to the boundary. As the boundary $|\vec{K}_\perp| = E$ is approached, ϕ becomes ill-defined and $\alpha = \theta_b - \pi$ defines the Fermi arc touching-point. This is consistent with the behavior shown in Fig. 1(b)–(c) of the main text.

To analytically derive the direction in which ϕ winds, consider momenta close to the boundary, such that $k_z^\pm = \pm\delta k_z$

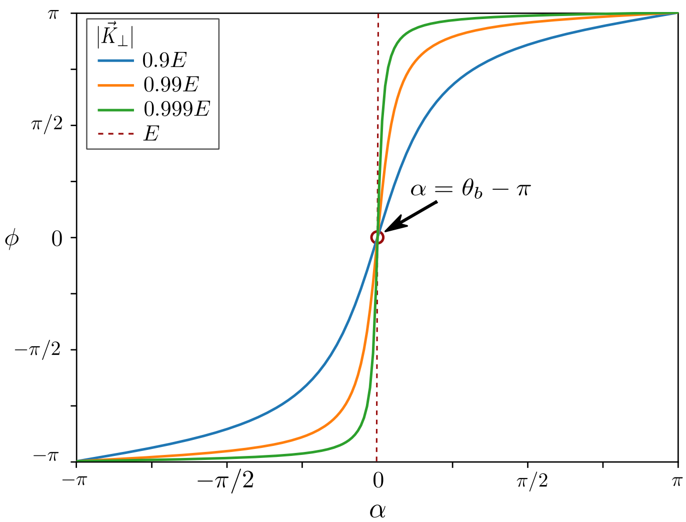

FIG. S1: Reflection phase ϕ versus α (the polar angle in the two-dimensional k-space of the incident beam), for $E = 1$, $\theta_b = \pi$, and different values of $|\vec{K}_\perp|$ close to the Weyl cone boundary. The Fermi arc touching-point occurs at $\alpha = 0$. Exactly at the boundary ($|\vec{K}_\perp| = E$), Eq. (S2) states that $\phi = \pi (\text{mod} 2\pi)$ for all $\alpha \neq 0$ and is undefined at $\alpha = 0$ (being a step function).

where δk_z is a small positive number. Let $q = \delta k_z/E$, and expand η_- up to linear order in q:

$$\eta_- = \sqrt{\frac{1+q}{1-q}} \approx 1+q, \qquad \eta_-^2 \approx 1+2q. \tag{S3}$$

Then the reflection coefficient is

$$\begin{aligned} e^{i\phi} &= -\frac{1+\eta_- e^{i\beta}}{\eta_- + e^{i\beta}} \\ &= -1 - \frac{2iq\sin\beta}{1+\cos\beta} + O(q^2), \end{aligned} \tag{S4}$$

where $\beta = \alpha - \theta_b$. Hence, to leading order,

$$\sin\phi \approx -\frac{2q\sin\beta}{1+\cos\beta}. \tag{S5}$$

At exactly $\beta = \pm\pi$, the denominator diverges and the approximation breaks down. For small angle deviations, $\beta = \pi + \delta\beta$, we find that $\sin\phi \approx 2q\sin(\delta\beta)$, so that $\delta\phi$ switches sign with $\delta\beta$. Note that $q > 0$ for the upper cone, and $q < 0$ for the lower cone, so the two cones have opposite windings.

B. Simple derivation of gaussian beam shifts

Let f be a function of the in-plane momenta $\vec{k}_\perp = (k_x, k_y)$. We take a gaussian beam of the form

$$\Psi = \frac{1}{2\pi\Delta_x\Delta_y}\int_{-\infty}^{\infty} dk_x dk_y\, e^{-\frac{(k_x-K_x)^2}{2\Delta_x^2}} e^{-\frac{(k_y-K_y)^2}{2\Delta_y^2}} e^{if(x,y,k_x,k_y)} e^{ik_x x + ik_y y}. \tag{S6}$$

To find the center of this beam, expand $f(x,y,k_x,k_y)$ about the mean wave-vector $\vec{K}_\perp = (K_x, K_y)$ as

$$f(x,y,k_x,k_y) \approx f(x,y,K_x,K_y) + \frac{\partial f}{\partial k_x}\Big|_{\vec{K}_\perp}(k_x - K_x) + \frac{\partial f}{\partial k_y}\Big|_{\vec{K}_\perp}(k_y - K_y). \tag{S7}$$

Here, only terms up to first order are retained. The integral (S6) can be written as

$$\Psi = C\int_{-\infty}^{\infty} dk_x\, \xi(k_x) e^{ik_x x}\int_{-\infty}^{\infty} dk_y\, \xi(k_y) e^{ik_y y} \tag{S8}$$

where

$$C = \frac{\exp[if(x,y,K_x,K_y)]}{2\pi\Delta_x\Delta_y}, \quad \xi(k_s) = \exp(-\frac{(k_s-K_s)^2}{2\Delta_s^2})\exp(i\frac{\partial f}{\partial k_s}\Big|_{\vec{K}_\perp}(k_s - K_s)). \tag{S9}$$

Evaluating the integrals, we obtain

$$\Psi = \exp\Big(if + iK_x x + iK_y y\Big)\exp\left[-\frac{\Delta_x^2}{2}\left(x + \frac{\partial f}{\partial k_x}\right)^2\right]\exp\left[-\frac{\Delta_y^2}{2}\left(x + \frac{\partial f}{\partial k_y}\right)^2\right]. \tag{S10}$$

We find that the probability amplitude $|\Psi|^2$ is a gaussian in real space, centered at

$$\vec{R} = \left[-\frac{\partial f}{\partial k_x}, -\frac{\partial f}{\partial k_y}\right]_{\vec{k}_\perp = \vec{K}_\perp}. \tag{S11}$$

For the particular case of Eq. (1) of the main text, the two components of the incident beam are centered at $(0,0)$ and $\big(-\partial_{k_x}\alpha, -\partial_{k_y}\alpha\big)_{\vec{k}_\perp = \vec{K}_\perp}$ and the center of the beam is calculated by taking weighted averages over the pre-factors:

$$\vec{R}_i = \left(-\frac{\eta_-^2}{1+\eta_-^2}\nabla_{\vec{k}_\perp}\alpha\right)_{\vec{k}_\perp = \vec{K}_\perp}, \tag{S12}$$

where, as in the main text,

$$\alpha = \tan^{-1}\left(\frac{k_y}{k_x}\right), \quad \eta_{\pm} = \sqrt{\frac{E - vk_z^{\pm}}{E + vk_z^{\pm}}}, \tag{S13}$$

$$k_z^{\pm} = \pm\sqrt{(E/v)^2 - |\vec{k}_{\perp}|^2}. \tag{S14}$$

Similarly, the reflected beam is centered at

$$\vec{R}_r = \left(-\frac{1}{1+\eta_+^2}\nabla_{\vec{k}_\perp}\phi - \frac{\eta_+^2}{1+\eta_+^2}\nabla_{\vec{k}_\perp}(\alpha+\phi)\right)_{\vec{k}_\perp=\vec{K}_\perp}. \tag{S15}$$

The shift is given by their difference:

$$\vec{\Delta}(\vec{K}_\perp) = \left(-\nabla_{\vec{k}_\perp}\phi + \left(\frac{\eta_-^2}{1+\eta_-^2} - \frac{\eta_+^2}{1+\eta_+^2}\right)\nabla_{\vec{k}_\perp}\alpha\right)_{\vec{k}_\perp=\vec{K}_\perp}. \tag{S16}$$

Using the equality $\eta_+ = 1/\eta_-$ yields Eq. (6) of the main text.

C. Non-Gaussian beams and gauge invariance

In this section, we show that the same beam shift formulas can be derived even if the Gaussian envelope approximation is relaxed. This derivation also shows that even though the reflection coefficient ϕ depends on the gauge choice used in the definition of the eigenfunctions [e.g., Eq. (1) of the main text], the beam shift $\vec{\Delta}$ is a physical quantity that is gauge invariant. The beam shifts are derived in terms of geometrical connections defined using the spinors of the incident and reflected beams.

Let $g(\vec{k}_\perp)$ be a real valued function peaked at $\vec{k}_\perp = \vec{K}_\perp$. The incident and reflected beam can be written as

$$\Psi_i(\vec{r},\vec{K}_\perp) = \int d\vec{k}_\perp\, g(\vec{k}_\perp - \vec{K}_\perp)\, \psi_i(\vec{k}_\perp)\, e^{i\vec{k}_\perp\cdot\vec{r}_\perp + ik_z^- z} \tag{S17}$$

$$\Psi_r(\vec{r},\vec{K}_\perp) = \int d\vec{k}_\perp\, g(\vec{k}_\perp - \vec{K}_\perp)\, \mathrm{r}(\vec{k}_\perp)\, \psi_r(\vec{k}_\perp) e^{i\vec{k}_\perp\cdot\vec{r}_\perp + ik_z^+ z}. \tag{S18}$$

Here, $\mathrm{r}(\vec{k}_\perp) = e^{i\phi(\vec{k}_\perp)}$ is the reflection coefficient. To track the peak of the wavepacket, we calculate the probability amplitude at the interface $z = 0$:

$$\left|\Psi_{i(r)}(\vec{K}_\perp,\vec{r}_\perp)\right|^2 = \int d\vec{k}_\perp d\vec{k}'_\perp\, g_F(\vec{k}_\perp,\vec{k}'_\perp,\vec{K}_\perp)\, e^{i\theta_{i(r)}(\vec{k}_\perp,\vec{k}'_\perp)} \tag{S19}$$

where

$$g_F(\vec{k}_\perp,\vec{k}'_\perp,\vec{K}_\perp) = g(\vec{k}_\perp,\vec{K}_\perp)g(\vec{k}'_\perp,\vec{K}_\perp), \tag{S20}$$

$$\theta_i(\vec{k}_\perp,\vec{k}'_\perp,\vec{r}) = -i\log\left\langle\psi_i(\vec{k}_\perp)\middle|\,\psi_i(\vec{k}'_\perp)\right\rangle + (\vec{k}_\perp - \vec{k}'_\perp)\cdot\vec{r} \tag{S21}$$

$$\theta_r(\vec{k}_\perp,\vec{k}'_\perp,\vec{r}) = -i\log\left\langle\psi_r(\vec{k}_\perp)\,\middle|\psi_r(\vec{k}'_\perp)\right\rangle + (\vec{k}_\perp - \vec{k}'_\perp)\cdot\vec{r} + \phi(\vec{k}_\perp) - \phi(\vec{k}'_\perp). \tag{S22}$$

We have used Dirac's bra-ket notation to express the various k-space integrals. The peak of the probability amplitude in real space is the stationary point $\vec{R}$ determined by

$$\nabla_{\vec{k}_\perp}\theta_{i(r)}(\vec{k}_\perp,\vec{k}'_\perp,\vec{R}_{i(r)})\Big|_{\vec{K}_\perp} = 0 \tag{S23}$$

This gives the peaks of the incident and reflected beams:

$$\vec{R}_i = \vec{\mathcal{A}}_i(\vec{K}_\perp) \tag{S24}$$

$$\vec{R}_r = \vec{\mathcal{A}}_r(\vec{K}_\perp) - \nabla_{\vec{k}_\perp}\phi(\vec{k}_\perp)|_{\vec{K}_\perp}. \tag{S25}$$

Here,

$$\vec{\mathcal{A}}_{i(r)}(\vec{k}_\perp) = i\Big\langle \psi_{i(r)}(\vec{k}_\perp)\Big|\nabla_{\vec{k}_\perp}\Big|\psi_{i(r)}(\vec{k}_\perp)\Big\rangle \tag{S26}$$

is the Berry connection for the incident (reflected) wave. By explicit calculation using the eigenstates of Weyl Hamiltonian, we obtain

$$\vec{\mathcal{A}}_i(\vec{k}_\perp) = -\frac{\eta_-^2}{\eta_-^2+1}\nabla_{\vec{k}_\perp}\alpha \tag{S27}$$

$$\vec{\mathcal{A}}_r(\vec{k}_\perp) = -\frac{\eta_+^2}{\eta_+^2+1}\nabla_{\vec{k}_\perp}\alpha. \tag{S28}$$

The shift is then given by

$$\vec{\Delta}(\vec{K}_\perp) = \vec{R}_r - \vec{R}_i = \vec{\mathcal{A}}_r(\vec{K}_\perp) - \vec{\mathcal{A}}_i(\vec{K}_\perp) - \nabla_{\vec{k}_\perp}\phi(\vec{k}_\perp)|_{\vec{K}_\perp} \tag{S29}$$

$$= \left(\frac{\eta_-^2-1}{\eta_-^2+1}\nabla_{\vec{k}_\perp}\alpha - \nabla_{\vec{k}_\perp}\phi\right)_{\vec{K}_\perp}. \tag{S30}$$

We have used the fact that $\eta_- = 1/\eta_+$. Eq. (S30) shows that Eq. 6 of the main text is valid for any shape of incident beam as long as the beam profile remains a real function peaked at a single point in real space. This in turn implies that the neglected higher order terms, which generally cause a change of the beam profile, will not change the calculated shift even upon multiple reflections.

Now consider boundary conditions of the form

$$\mathrm{M}(\vec{k}_\perp)\left[\psi_i(\vec{k}_\perp) + r(\vec{k}_\perp)\psi_r(\vec{k}_\perp)\right] = 0, \tag{S31}$$

where $\mathrm{M}(\vec{k}_\perp)$ is a 2×2 matrix characterizing the boundary. The reflection phase can be written as

$$\phi(\vec{k}_\perp) = i\log[\mathrm{M}\psi_r(\vec{k}_\perp)] - i\log[\mathrm{M}\psi_i(\vec{k}_\perp)]. \tag{S32}$$

The derivative is

$$\nabla\phi = i\frac{\nabla\mathrm{M}\psi_r}{\mathrm{M}\psi_r} - i\frac{\nabla\mathrm{M}\psi_i}{\mathrm{M}\psi_i}. \tag{S33}$$

We define two new objects

$$\psi_{i(r)}^\theta = \mathrm{M}\psi_{i(r)}, \tag{S34}$$

which are normalized as $\langle\psi_{i(r)}^\theta(\vec{k}_\perp)|\psi_{i(r)}^\theta(\vec{k}_\perp)\rangle = 1$. Then Eq. (S33) reads

$$\nabla\phi = \Big\langle\psi_r^\theta(\vec{k})\Big|i\nabla_{\vec{k}}\Big|\psi_r^\theta(\vec{k})\Big\rangle - \Big\langle\psi_i^\theta(\vec{k})\Big|i\nabla_{\vec{k}}\Big|\psi_i^\theta(\vec{k})\Big\rangle, \tag{S35}$$

which is the difference between two geometric (non-Berry) connections. These geometric connections are related to the parallel transport determined by the boundary condition.

Although both $\vec{R}_i$ and $\vec{R}_r$ are gauge dependent (which amounts to a different choice of origin for the individual waves), their difference is gauge invariant. When

$$\psi_{i(r)}(\vec{k}_\perp) \to \psi_{i(r)}(\vec{k}_\perp)\exp(i\chi_{i(r)}(\vec{k}_\perp)), \tag{S36}$$

we find that

$$\vec{\mathcal{A}}_{i(r)}(\vec{k}_\perp) \to \vec{\mathcal{A}}_{i(r)}(\vec{k}_\perp) - \nabla_{\vec{k}_\perp}\chi(\vec{k}_\perp) \tag{S37}$$

$$\nabla_{\vec{k}_\perp}\phi(\vec{k}_\perp) \to \nabla_{\vec{k}_\perp}\phi(\vec{k}_\perp) - \nabla_{\vec{k}_\perp}\chi_r(\vec{k}_\perp) + \nabla_{\vec{k}_\perp}\chi_i(\vec{k}_\perp). \tag{S38}$$

Hence, the shift given by Eq. (S30) is gauge invariant.

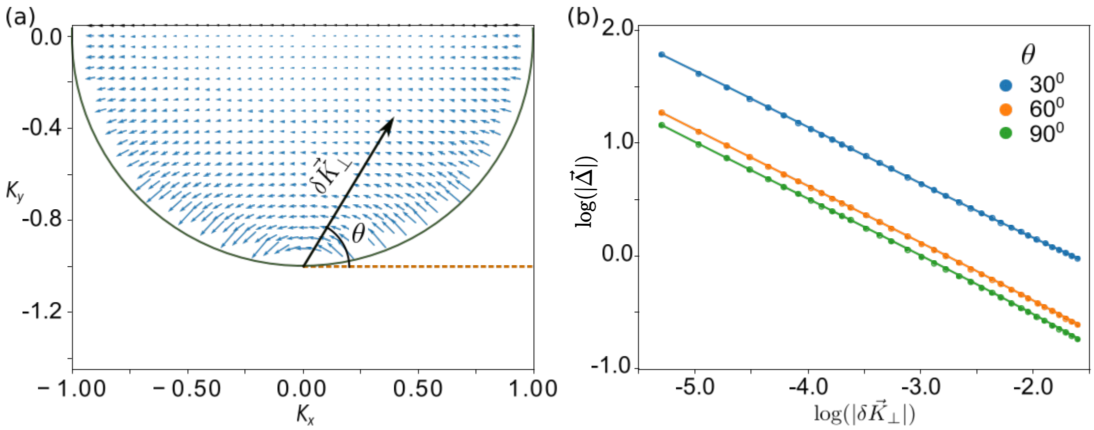

FIG. S2: (a) Zoomed-in image of the shift vector $\vec{\Delta}$ close to the Fermi arc touching-point. (b) Log-log plot of the magnitude of the shift vector in different directions away from the Fermi arc touching-point. The straight lines show numerical least squares fits, which indicate that the magnitudes indeed scale as $|\vec{\Delta}| \sim |\delta\vec{K}_\perp|^{-1/2}$.

The shift itself is given by

$$\vec{\Delta}(\vec{K}_\perp) = \left(\frac{\eta_-^2 - 1}{\eta_-^2 + 1}\nabla_{\vec{k}_\perp}\alpha(\vec{k}_\perp) - \nabla_{\vec{k}_\perp}\phi(\vec{k}_\perp)\right)_{\vec{k}_\perp = \vec{K}_\perp}. \tag{S39}$$

The reflection coefficient is given by

$$r = e^{i\phi} = -\frac{1 + \eta_- e^{i\beta}}{\eta_- + e^{i\beta}}, \tag{S40}$$

where $\beta(\vec{k}_\perp) = \alpha(\vec{k}_\perp) - \theta_b$. Therefore,

$$\nabla\phi = -i\frac{\nabla r(\vec{k}_\perp)}{r(\vec{k}_\perp)} \tag{S41}$$

$$= -\frac{i}{r}\frac{ie^{i\beta}(\eta_-^2 - 1)(\nabla\beta) + (e^{2i\beta} - 1)(\nabla\eta_-)}{(\eta_- + e^{i\beta})^2} \tag{S42}$$

$$= \frac{(\eta_-^2 - 1)(\nabla\beta) + 2\sin\beta(\nabla\eta_-)}{1 + \eta_-^2 + 2\eta_-\cos\beta}, \tag{S43}$$

and

$$\nabla\eta_- = \frac{-E}{\eta(E + k_z^-)^2}\frac{\vec{k}_\perp}{|k_z^-(\vec{k}_\perp)|} \tag{S44}$$

$$\nabla\beta = \nabla\alpha = (-k_y, k_x)/|\vec{k}_\perp|^2. \tag{S45}$$

Putting everything together, we obtain the explicit formula

$$\vec{\Delta}(\vec{K}_\perp) = \left[\frac{\eta_-^2(\vec{K}_\perp) - 1}{\eta_-^2(\vec{K}_\perp) + 1} + \frac{k_z^-(\vec{K}_\perp)}{E + |\vec{K}_\perp|\cos\beta(\vec{K}_\perp)}\right]\frac{1}{|\vec{K}_\perp|^2}(-K_y, K_x) + \frac{E\sin\beta(\vec{K}_\perp)}{|\vec{K}_\perp|E + |\vec{K}_\perp|^2\cos\beta(\vec{K}_\perp)}\frac{\vec{K}_\perp}{|k_z(\vec{K}_\perp)|}. \tag{S46}$$

D. Inverse square root scaling of the beam displacement

Fig. S2 shows the inverse square-root scaling of the magnitude of the shift near the Fermi arc touching-point $\vec{K}_{\rm fa}$. As mentioned in the main text, the vortex structure near the Fermi arc touching-point is due to the gradient of the reflection phase, as explicitly shown in Fig. S3. The scaling can be verified by expanding the gradient of reflection

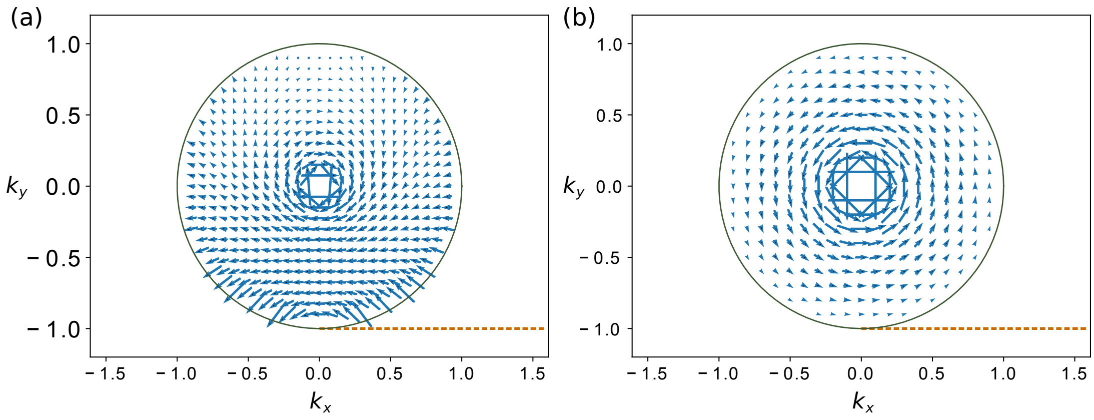

FIG. S3: Momentum dependence of the vector fields (a) $-\nabla\phi$ and (b) $\nabla\alpha$, for $\theta_b = \pi/2$. The half-vortex structure near the Fermi arc touching-point is evidently due to the gradient of ϕ. Note that $-\nabla\phi$ and $\nabla\alpha$ circulate in opposite directions around the origin.

phase about the Fermi arc touching-point. The latter is derived by requiring the penetration constant of the Fermi arc surface state to vanish, which yields

$$\vec{K}_{\rm fa} = \Big(- E\cos(\theta_b), -E\sin(\theta_b)\Big). \tag{S47}$$

We define $\vec{k}_\perp = \vec{K}_{\rm fa} + \delta\vec{k}$, where $\delta\vec{k} = (\delta k_x, \delta k_y)$ is the wave-vector measured from the Fermi arc touching-point. The shift $\vec{\Delta}$, given by (S46), is to be expanded up to linear order in $\delta\vec{k}$.

We can expand k_z^- in linear order as follows:

$$k_z^- \approx -\sqrt{2E[\delta k_x\cos(\theta_b) + \delta k_y\sin(\theta_b)]} = -Eq \tag{S48}$$

where

$$q = \sqrt{\frac{2[\delta k_x\cos(\theta_b) + \delta k_y\sin(\theta_b)]}{E}}. \tag{S49}$$

And from the definition of α we have

$$\cos(\alpha) \approx \frac{p\sin(\theta_b)}{E} - \cos(\theta_b), \;\; \sin(\alpha) \approx -\frac{p\cos(\theta_b)}{E} - \sin(\theta_b), \tag{S50}$$

where

$$p = \delta k_x\sin(\theta_b) - \delta k_y\cos(\theta_b). \tag{S51}$$

and this gives

$$\sin\beta \approx -\frac{p}{E}, \;\; \cos\beta \approx -1 \tag{S52}$$

where $\beta = \alpha - \theta_b$. Now, from (S43) and (S46) we have

$$\begin{aligned}\nabla\phi \approx & -\frac{-q}{(1-\sqrt{1-q^2})}\frac{1}{E^2(1-q^2)}(-\delta k_y + E\sin\theta_b, \delta k_x - E\cos\theta_b)\\ & -\frac{p}{E^2(\sqrt{1-q^2}-(1-q^2))}\frac{1}{Eq}(\delta k_x - E\cos\theta_b, \delta k_y - E\sin\theta_b).\end{aligned} \tag{S53}$$

which expanding up to linear order in q simplifies to

$$\nabla\phi \approx -\frac{2}{E^2}(\frac{1}{q}+q)(-\delta k_y + E\sin\theta_b, \delta k_x - E\cos\theta_b) - \frac{2p}{E^3q^3}(\delta k_x - E\cos\theta_b, \delta k_y - E\sin\theta_b) \tag{S54}$$

Noting that $p/q^3 \sim 1/q$, it is readily seen that the leading order term scales as $1/q$.

E. Derivation of the shift for the quadratic Hamiltonian

The quadratic Hamiltonian

$$H = v\begin{bmatrix} -k_y & \gamma(k_x^2 - m) - ik_z \\ \gamma(k_x^2 - m) + ik_z & k_y \end{bmatrix} \tag{S55}$$

has dispersion relation

$$E = \pm v\sqrt{(k_x^2 - m)^2 + k_y^2 + k_z^2}. \tag{S56}$$

This can exhibit either paired Weyl points or complete band-gap, depending on the choice of m. In the region $z > 0$, we set $m = m_0 > 0$, so that there is a pair of Weyl points at $\vec{k} = [\pm\sqrt{m_0}, 0, 0]$; for small values of $|E|$, there are two distinct Weyl cones which merge as $|E|$ increases. In the region $z < 0$, we set $m = -m_1 < 0$ so that there is a complete band gap in the range $|E| < v\gamma|m_1|$. In the Weyl medium, for incident and reflected plane waves, the eigenvectors reads

$$\Psi_i = \frac{1}{\sqrt{1+\eta^2}}\begin{bmatrix} e^{-i\alpha_-} \\ \eta \end{bmatrix}, \quad \Psi_r = \frac{e^{i\phi}}{\sqrt{1+\eta^2}}\begin{bmatrix} e^{-i\alpha_+} \\ \eta \end{bmatrix}, \tag{S57}$$

where

$$\begin{aligned} \alpha_\pm &= \tan^{-1}\left(\frac{k_z^\pm}{\gamma(k_x^2 - m_0)}\right), \quad \eta = \sqrt{\frac{E + vk_y}{E - vk_y}}, \\ k_z^\pm &= \pm\sqrt{(E/v)^2 - \gamma^2(k_x^2 - m_0)^2 - k_y^2}, \end{aligned} \tag{S58}$$

where as before $k_z < 0$ ($k_z > 0$) branch chosen for the incident (reflected) wave.

The reflection amplitude $e^{i\phi}$ is calculated by matching the total incident and reflected envelope functions at $z = 0$ plane with the evanescent wave in the band-gap medium given by

$$\psi_t = \frac{t}{N_t}\begin{bmatrix} E/v - k_y \\ \gamma(k_x^2 + m_1) + \kappa \end{bmatrix} e^{ik_x x + ik_y y + \kappa z}, \tag{S59}$$

where $\kappa = \sqrt{\gamma^2(k_x^2 + m_1)^2 + k_y^2 - (E/v)^2}$ is the inverse decay length of the evanescent field, t is the transmission coefficient and N_t is a normalization factor. Equating $\psi_i + \psi_r = \psi_t$ at $z = 0$ for all x and y, the reflection coefficient $e^{i\phi}$ is calculated:

$$e^{i\phi} = \frac{\eta(E - vk_y) - [v\gamma(k_x^2 + m_1) + v\kappa]e^{-i\alpha_-}}{e^{-i\alpha_+}[v\gamma(k_x^2 + m_1) + v\kappa] - \eta(E - vk_y)} \tag{S60}$$

The spatial shift in the reflected beam can be calculated in a manner similar to the previous case, which gives

$$\vec{\Delta}(\vec{K}_\perp) = \left(-\nabla_{\vec{k}_\perp}\phi - \frac{2}{\eta^2 + 1}\nabla_{\vec{k}_\perp}\alpha_-\right)_{\vec{k}_\perp = \vec{K}_\perp}. \tag{S61}$$

The results are shown in Fig. 3 of the main text.

F. Consecutive reflections in a thin film geometry

Consider a film of Weyl medium of thickness $2L$, within the space $|z| < L$ bounded above and below by a gapped medium. In this geometry, a beam in the Weyl medium will reflect repeatedly off the two parallel surfaces, much like a bouncing-ball trajectory within a waveguide, as shown in Fig. S4(a).

As the beam reflects consecutively off the bottom and top surfaces of the film, the beams displacements accumulate instead of cancelling. Fig. S4(b)–(c) plots the numerically-calculated beam shift over two consecutive reflections, using the quadratic Weyl Hamiltonian with continuity boundary conditions at $|z| = L$. The shift from the upper surface can be found by replacing $k_z^\pm \to k_z^\mp$ and $\kappa \to -\kappa$ in the previous equations.

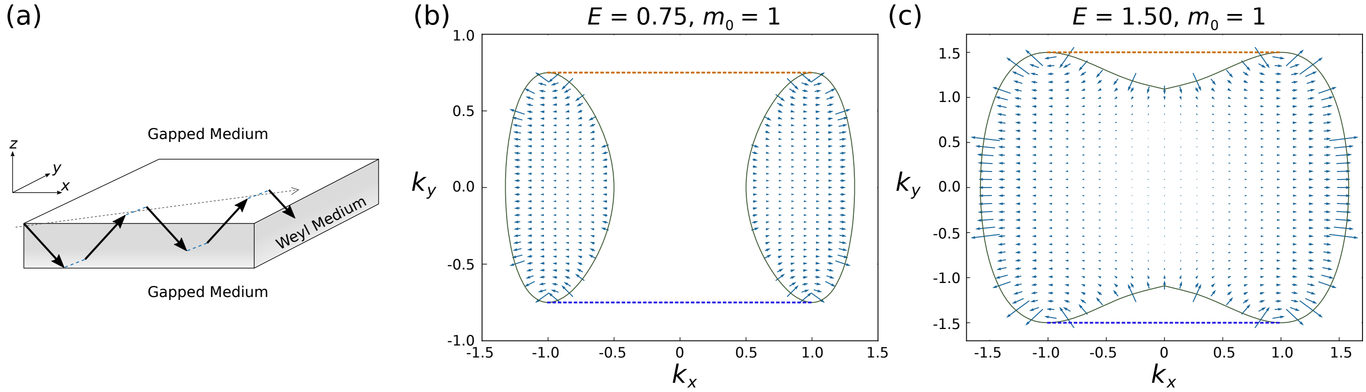

FIG. S4: (a) Schematic of a beam bouncing within a thin film geometry. (b)–(c) Beam shift versus incident in-plane momentum, over two consecutive reflections in the thin film. The orange (blue) dashes show the Fermi arc on the bottom (top) surface.

In explicit terms, we take the Hamiltonian

$$H = \begin{bmatrix} -k_y & (k_x^2 - m) - ik_z \\ (k_x^2 - m) + ik_z & k_y \end{bmatrix}, \quad m = \begin{cases} m_0 > 0, & |z| \le L \text{ (Weyl medium)} \\ -m_1, & |z| > L \text{ (gapped medium)}. \end{cases} \tag{S62}$$

Inside the Weyl semimetal, we look for states $\propto e^{i\vec{k}_\perp \cdot \vec{r}_\perp + ik_z^\pm z}$ with $\vec{k}_\perp = (k_x, k_y)$ and $\vec{r}_\perp = (x, y)$. We focus on a fixed energy E, whose bulk states read

$$\begin{aligned} \psi_\pm^{\mathrm{w}}(\vec{k}_\perp, \vec{r}_\perp, z) &= \frac{1}{\sqrt{1+\eta^2}} \begin{bmatrix} e^{i\alpha_\mp} \\ \eta \end{bmatrix} e^{i\vec{k}_\perp \cdot \vec{r}_\perp + ik_z^\pm z} \\ \eta &= \sqrt{\frac{E + k_y}{E - k_y}} \\ \alpha_\pm &= \arctan\left(\frac{k_z^\pm}{k_x^2 - m_0}\right) \\ k_z^\pm &= \pm\sqrt{E^2 - (k_x^2 - m_0)^2 - k_y^2}. \end{aligned} \tag{S63}$$

Here, $\psi_\pm^{\mathrm{w}}(\vec{k}_\perp, \vec{r}_\perp, z)$ propagates to the upper/lower surface $z = \pm L$. We assume that the energy lies within the gap of the external medium. In the $z > L$ ($z < -L$) region, the solution has the decaying form

$$\psi_\pm^{\mathrm{evs}}(\vec{k}_\perp, \vec{r}_\perp, z) \propto \begin{bmatrix} E - k_y \\ k_x^2 + m_1 \mp \kappa \end{bmatrix} e^{ik_x x + ik_y \mp \kappa z}. \tag{S64}$$

This wave function is not normalized, and due to energy conservation,

$$\kappa = \sqrt{(k_x^2 + m_1)^2 - (k_x^2 - m_0)^2}. \tag{S65}$$

At the interface $z = \pm L$, the incident wave $\psi_\pm^{\mathrm{w}}$, the reflected wave $\psi_\mp^{\mathrm{w}}$, and the evanescent wave $\psi_\pm^{\mathrm{evs}}$ must match:

$$\psi_\pm^{\mathrm{w}}(\vec{k}_\perp, \vec{r}_\perp, \pm L) + \mathrm{r}_\pm(\vec{k}_\perp)\psi_\mp^{\mathrm{w}}(\vec{k}_\perp, \vec{r}_\perp, \pm L) = \mathrm{t}_\pm(\vec{k}_\perp)\psi_\pm^{\mathrm{evs}}(\vec{k}_\perp, \vec{r}_\perp, \pm L), \tag{S66}$$

where $\mathrm{r}_\pm(\vec{k}_\perp)$ and $\mathrm{t}_\pm(\vec{k}_\perp)$ are reflection and transmission coefficients at $z = \pm L$. By multiplying $(k_x^2 + m_1 \mp \kappa, -E + k_y)$ to both sides of the equation, we obtain the total reflection coefficient

$$\mathrm{r}_\pm(\vec{k}) = -\frac{e^{i\alpha_\mp}(k_x^2 + m_1 \mp \kappa) - \sqrt{E^2 - k_y^2}}{e^{i\alpha_\pm}(k_x^2 + m_1 \mp \kappa) - \sqrt{E^2 - k_y^2}} \equiv -\exp[i\phi_\pm(\vec{k}_\perp)]. \tag{S67}$$

For wave packets composed by $\psi_\pm^{\mathrm{w}}$, the shift between the total reflected wave and the incident wave in real space at the interface $z = \pm L$ is

$$\vec{\Delta}_\pm(\vec{k}_\perp) = \vec{A}_\mp(\vec{k}_\perp) - \vec{A}_\pm(\vec{k}_\perp) - \nabla_{\vec{k}_\perp}\phi_\pm(\vec{k}_\perp) \tag{S68}$$

where $\vec{A}_\pm(\vec{k}_\perp) = i\langle\psi^{\mathrm{w}}_\pm(\vec{k}_\perp)|\nabla_{\vec{k}_\perp}|\psi^{\mathrm{w}}_\pm(\vec{k}_\perp)\rangle$ is the Berry connection for the incident/reflected state. Since $\vec{A}_+(\vec{k}_\perp) - \vec{A}_-(\vec{k}_\perp)$ and $\vec{A}_-(\vec{k}_\perp) - \vec{A}_+(\vec{k}_\perp)$ cancel, after two consecutive reflections between opposite surfaces $z = \pm L$, the total shift is

$$\vec{\Delta}_{\mathrm{tot}}(\vec{k}_\perp) = \vec{\Delta}_+(\vec{k}_\perp) + \vec{\Delta}_-(\vec{k}_\perp) = -\nabla_{\vec{k}_\perp}\phi_+(\vec{k}_\perp) - \nabla_{\vec{k}_\perp}\phi_-(\vec{k}_\perp). \tag{S69}$$

The resulting map of the shift is shown in Fig. S4.

G. Python scripts

Python scripts for producing the plots in the main text and this set of Supplemental Notes may be downloaded from ⟨https://doi.org/10.21979/N9/CVSM4Z⟩.